Steel and Composite Structures, Vol. 8, No. 1 (2008) 19-34
DOI: http://dx.doi.org/10.12989/scs.2008.8.1.019

Analysis of restrained steel beams subjected to heating and cooling Part II: Validation and parametric studies

Shi-Xiong Guo and Guo-Qiang Li†

Department of Structural Engineering Tongji University, 1239 Siping Road, Shanghai 200092 P. R. China

(Received August 0, 2007, Accepted October 0, 2007)

Abstract. This paper presents the results of a validation and parametric study for the theory presented in the companion paper. The parameters investigated include the stiffness of axial and rotational restraints, load ratio, depth-span ratio of the beam, the yield strength of steel, load type and the temperature distribution in the crosssection of the beam.

Keywords : fire-resistance; steel structure; catenary action; large deflection.

1. Validation study for restrained steel beams subjected to increasing temperature

The validation study will be based on the results of Liu *et al.* (2002) who carried out a series of experiments to investigate the behaviour of restrained steel beams in fire condition. In the experiments, the effects of axial and rotational restraints were considered, and catenary action was observed.

The testing assembly (elevation) is shown in Fig. 1. The axial restraints on the test beam were applied by the fire-protected columns and its neighboring sub-frames. The cross-section of the beam was 178 × 102 × 19UB(S275). Except the top flange, which was wrapped with 15 mm thick ceramic fiber blanket, the rest of the beam was unprotected. The column, of section 152 × 152 × 30UC (S275), together with the connections were fully fire-protected. The temperature of the furnace was controlled to follow the ISO834 standard fire curve (ISO 1980). The temperature distribution and developments in the beams was measured and is shown in Fig. 2.

For specimens FUR29 and FUR31 in the experiment, the connections were flush-end plate of 10 mm thickness with M16 Grade 8.8 bolts, as shown in Fig. 3. According to Eurocode 3 (2003), the rotational stiffness of the connection is about 2.5×10^3 kNm/rad. The rotational stiffness of the columns to the beam is 1.49×10^4 kNm/rad. The bending stiffness of the test beam is 1.4×10^3 kNm/rad, giving the effective rotational stiffness of the restrained beam as 609 kNm/rad.

Based on Eqs. (9)~(13) in the companion paper (Li and Guo 2008), the deflection curve of the test beam can be expressed by

$$f_1(x) = \frac{\delta}{0.022L^3}(-0.1667x^3 + 0.0458Lx^2 + 0.0592L^2x) \qquad x \le 0.3L \tag{1a}$$

†Corresponding author, E-mail: gqli@mail.tongji.edu.cn

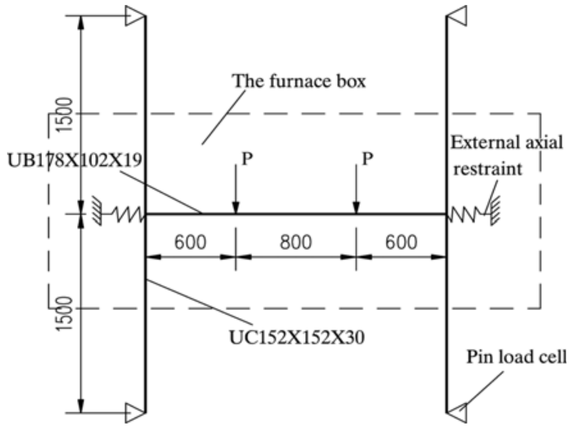

Fig. 1 Testing assembly (elevation)

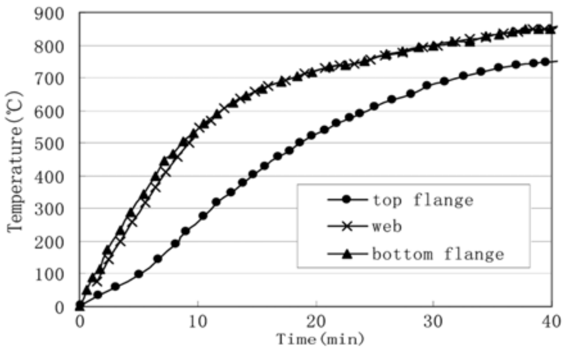

Fig. 2 Typical temperature distribution and developments in the test beams

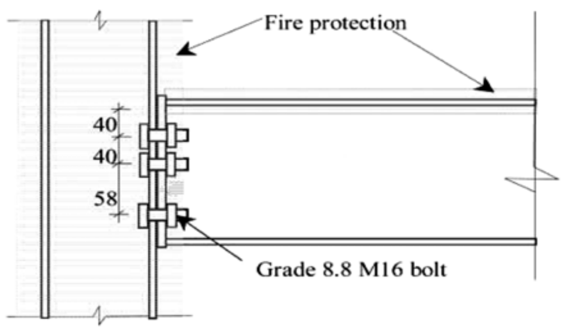

Fig. 3 Flush end-pate connection

$$f_2(x) = \frac{\delta}{0.022L^2}(-0.1042x^2 + 0.1042Lx - 0.0045L^2) \qquad 0.3L < x \leq 0.5L \qquad (1b)$$

where L is the span of the beam and δ is the deflection at the mid-span of the beam.

For specimens FUR29 and FUR31, the load ratio, which is defined as the ratio of load applied on a beam over the carrying capacity of the beam at ambient temperature, was 0.5, and the stiffness of the

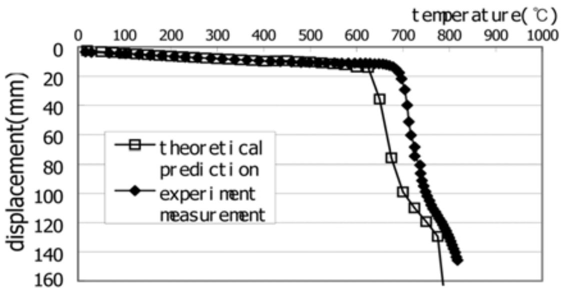

Fig. 4 Development of deflection of specimen FUR31

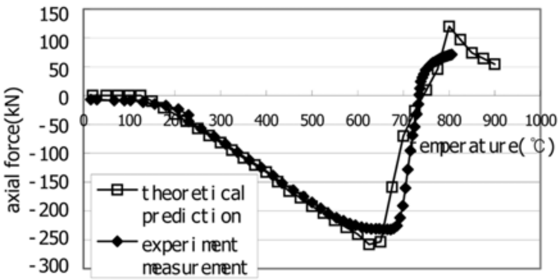

Fig. 5 Development of axial force of specimen FUR31

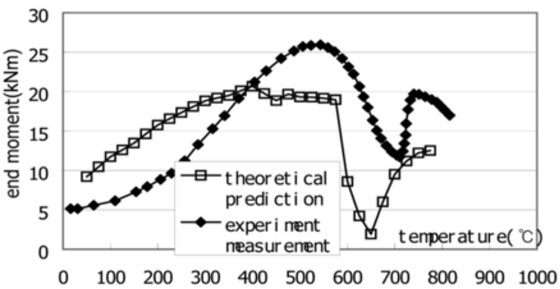

Fig. 6 Development of end moment of specimen FUR31

axial restraint was 62 kN/mm. Figs. 4~9 present various comparisons between measured and predicted results, in which Fig. 4 and Fig. 7 are deflections of specimens, Fig. 5 and Fig. 8 for axial forces, and Fig. 6 and Fig. 9 for bending moment at the ends of the beam. In all the illustrations, the temperature is that at the bottom flange of the beam.

From Figs. 4~9, it can be seen that the developments of deflections and axial forces of the beams are similar between the theoretical predictions and experimental measurements. However, the end moments of the specimens obtained by the theoretical analysis is smaller than those from experiments. The reason may be that in the experiments the temperatures at the ends of the beams were lower than at other place of the beams while in the theoretical analysis the temperatures are supposed to be uniformly distributed along the span of the beam. So the ends of the beams had higher stresses in the experiments than theoretically predicted.

Overall, the prediction of the behaviour of the specimens by the proposed theory is satisfactory.

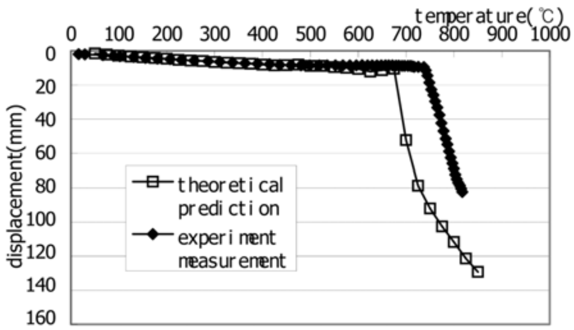

Fig. 7 Development of axial force of specimen FUR29

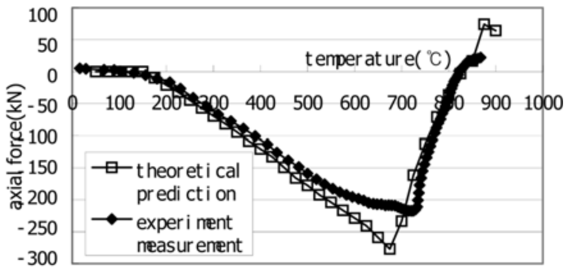

Fig. 8 Development of deflection specimen FUR29

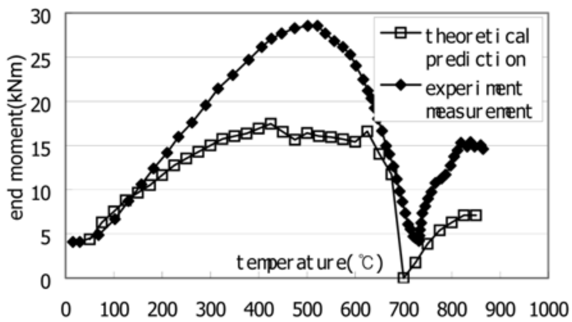

Fig. 9 Development of end moment of specimen FUR29

2. Parametric analysis for restrained steel beam subjected to increasing temperature

According to the theory in the companion paper (Li and Guo 2008), the parameters that affect the behaviour of restrained steel beam subjected to fire can be determined. Obviously, the axial restraint stiffness and load ratio will be the most important parameters. In addition, because the span-depth ratio of the beam and the stiffness of rotational restraints will influence the profile of deflection of restrained beams, so they are included in this investigation. On the other hand, temperature gradients in cross sections of different steel beams change widely, and it is difficult to get accurate temperature gradients in fire, which will complicate the analyses of restrained beams. Assuming uniform temperature distribution in cross section can simplify the analyses of restrained beams in fire, but the disparity of the results should be investigated. So effects of non-uniform temperature distribution in the cross-section are investigated too.

In order to understand the effects of above parameters, a group of restrained steel beams are studied. The sections of all the beams are 406 × 178 × 60UB. Unless otherwise specified, the default values of the parameters of these beams for parametric studies are the same as those of a reference beam, which is listed in Table 1.

2.1 Effects of axial restraint stiffness on the beam

One of the important factors affecting the behaviour of restrained steel beams is the axial stiffness of the restraints, which has been studied by some previous researchers (Huang and Tan 2002, Yin and Wang 2004). This section presents the results of a study using the theoretical method presented in the companion paper (Li and Guo 2008). The beams similar to the reference beam introduced in Table 1 are investigated, but the axial restraints are $k_a = 0.01\ k_b$, $0.02\ k_b$, $0.05\ k_b$, $0.1\ k_b$ and $0.15\ k_b$, respectively.

Based on Eqs. (9)~(13) in the companion paper (Li and Guo 2008), given the temperature distribution is uniform in the cross-section, the deflection curve of the uniformly loaded beam with rotation fully restrained at the ends can be derived as:

$$f(x) = 16\delta\left(\frac{x^4}{L^4} - \frac{2x^3}{L^3} + \frac{x^2}{L^2}\right) \tag{2}$$

where L is the span of the beam and δ the deflection at the mid-span of the beam.

The developments of deflections and axial forces of the restrained beams with various axial restraints are shown in Fig. 10 and Fig. 11 respectively. It can be seen that in stage I and stage II (please refer to Fig. 5 in the companion paper (Li and Guo 2008) for the definition of behaviour stages of a restrained beam in fire), the larger the axial restraint stiffness, the larger the deflection and the compressive axial force of the beam. When the compressive axial force is reduced to zero, the deflections of the beam with various axial restraint stiffness are close to each other. In stage III, the larger the axial restraint stiffness, the smaller the deflection of the beam, but the larger the tensile axial force in the beam. However, in stage IV when the beam has reached its tensile capacity, the developments of the deflections and tensile axial force of the beams with various axial restraints become close to each other again.

These phenomena can be explained by the equilibrium equation of the beam as:

$$M_{end} + M_{mid} - M_{eff} - F\delta = 0 \tag{3}$$

where M_{end} is the restraint moment at the end of the beam; M_{mid} is the resistant moment at the mid span; M_{eff} is the moment about the end caused by external load applied on the beam and F is the axial force in the beam.

F can be given by:

$$F = \left(\alpha L T - \lambda\frac{\delta^2}{L}\right)k_{e,\,a} \tag{4}$$

Table 1 Values of parameters of the reference beam

Axial restraint stiffness	Rotational restraint stiffness	Load ratio	Span	Load type	Temperature distribution
$0.1\ k_b$	∞	0.5	8 m	Uniform	Uniform

Note : k_b is the axial stiffness of a beam at ambient temperature

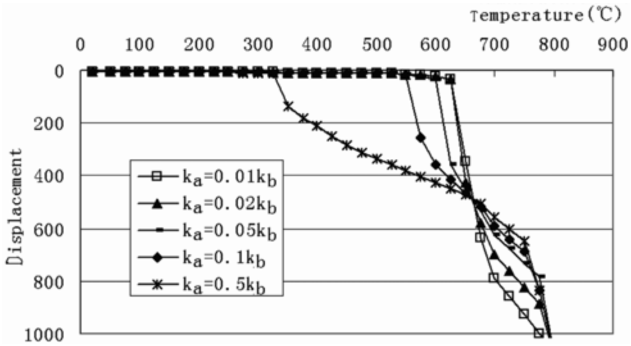

Fig. 10 Development of the beam with various axial restraints stiffness

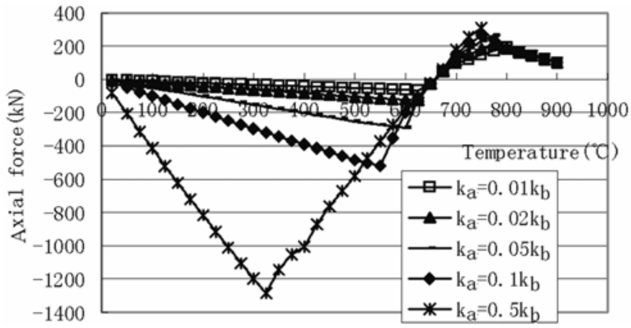

Fig. 11 Axial forces of the beam with various axial restraints

where α is the coefficient of thermal expansion; λ is a factor relevant to the shape of $f(x)$; $k_{e,a}$ is the effective axial stiffness.

In stage I, δ is small. According to Eq. (4), F is mainly determined by T and $k_{e,a}$. Obviously, the larger the axial restraint, the larger the value of F in compression. The larger F will cause earlier yield and P-δ effect, leading to larger deflections of the beam. At the end of stage II, the axial force is reduced to zero, but the bending moments at this point are independent of the axial restraint stiffness. So the deflections of the beam with various axial restraints are the same. In stage III, F becomes tension, which helps the beam to resist the applied load. Hence, for the beam with larger axial restraint stiffness, since F is larger, a smaller deflection will be needed to support the load. In stage IV, because F has reached the maximum gradually, which is the yield force of the cross-section of the beam, F is no longer related to the axial restraint stiffness, the behaviour of the restrained beam with various axial restraint stiffness becomes similar again.

2.2 Effects of rotational restraint stiffness

In order to investigate the effects of rotational restraint stiffness on the behaviour of restrained steel beams subjected to fire, the beams similar to the reference beam is analysed. The effective rotational stiffness of the beam (please refer to the companion paper (Li and Guo 2008) for the definition of the effective rotational stiffness), $k_{e,r} = 0$, $0.05EI/L$, $0.1EI/L$, $0.5EI/L$ and EI/L are used for the parametric studies.

Let $\gamma = \dfrac{k_{e,r}}{EI/L}$, the deflection of the beam with rotational restraints can be expressed as

$$f(x) = \frac{16\delta}{5-4}\left(\frac{x^4}{L^4} - 2\frac{x^3}{L^3} + \gamma\frac{x^2}{L^2} + (1-\gamma)\frac{x}{L}\right) \tag{5}$$

The developments of deflections and axial forces of the beams with various restraint stiffness are shown in Fig. 12 and Fig. 13, respectively. In Fig.12, it is shown that in stages I~III, the smaller is the rotational restraint stiffness, the earlier does the beam yield, and the larger is the deflection. However, in stage IV, the deflection of the beam with higher rotational restraint stiffness is larger than that with lower rotational stiffness. In Fig.13, it is shown that the higher the rotational restraint stiffness, the smaller are the maximum value of the axial compressive and tensile force. Another fact should be noticed is that the beams with the effective rotational stiffness higher than or equal $0.5EI/L$ have similar developments of deflections and axial forces.

In a beam, a smaller rotational restraint gives a smaller end bending moment, which will lead to a larger deflection. According to Eq. (3), larger deflection will cause larger additional moment by the axial force, which will result in earlier yielding of the beam. On the other hand, under the same load ratio, in fact, the beams with higher rotational restraint stiffness bearing higher external load, which leads to higher M_{eff}. Then in stages III and IV, according to Eq. (3), when M_{end} and M_{mid} are very small, higher tensile axial force F will be needed to resist higher M_{eff}. When the effective rotational stiffness reaches or exceeds $0.5EI/L$, the ends of the beam are approximately rigidly restrained, and the deflection profile and bending moment diagram is similar to that of beams with fixed ends. So their behaviours are close.

2.3 Effects of load ratio

In this study, the load ratios are Lr = 0.3, 0.5, 0.7 and 0.9. The developments of deflections and axial forces of the beam with various load ratios are shown in Fig. 14 and Fig. 15. Obviously, higher load induces larger deflection and moment, which leads to earlier yield. Because the beam with higher load yield earlier, the maximum value of axial compressive axial force is smaller. In stages III and IV, according to Eq.(3), higher load induces higher M_{eff}, which needs larger axial tensile force F to be resisted. An interesting fact is that though the load ratio is 0.9 and temperature has exceeded 600°C, the run away deflection does not occur, which indicts the important effect of centenary action in stages III and IV.

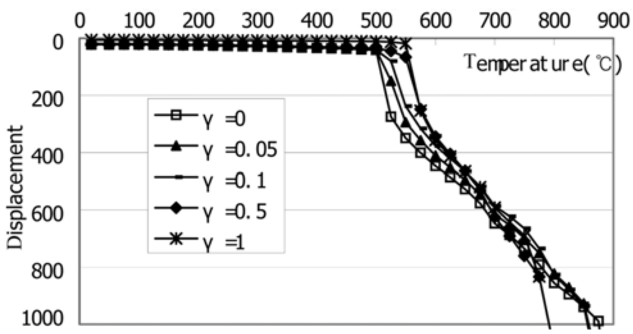

Fig. 12 Deflections of the beam with various rotational restraints

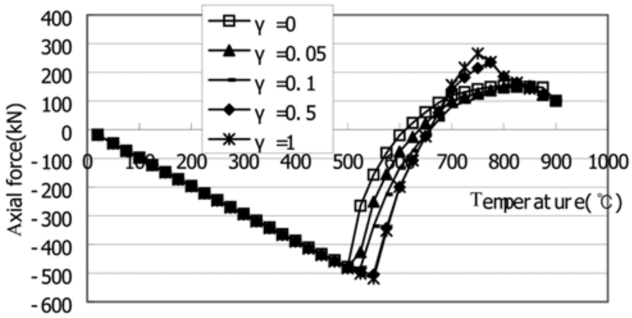

Fig. 13 Axial forces of the beam with various rotational restraints

2.4 Effects of beam depth-span ratio

In this study, the beam spans are 4 m, 6 m and 8 m, which gives the depth-span ratios of 1/10, 1/15 and 1/20 approximately. The stiffness of axial restraints is kept at 19.7kNm. Figs. 16 and 17 present the developments of deflections and axial forces of the beams.

Fig. 16 shows that the smaller is the depth-span ratio, the earlier does the beam yield. In stage I and II, the beam with smaller depth-span ratio has larger deflection and axial force. However, in stage III and IV, the beam with smaller depth-span ratio has smaller deflection and maximum value of the tension force.

In stage I, according to Eq. (4), the deflection is relatively small, and F is determined mainly by beam span L. Then the larger is L, the larger is F, which leads to the earlier yield of the beam. At the end of stage II, when F reduces to zero, according to Eq(3), because M_{mid}, M_{end}, M_{eff} in different beams are equal, so the temperature at which F equals to zero for different beams are equal, too. At the same temperature, Eq. (4) changes to $\alpha LT - \lambda\frac{\delta^2}{L} = 0$, which can be expressed as $\left(\frac{\delta}{L}\right)^2 = \frac{\alpha T}{L}$, so the values of δ / L of different beams are equal.

In stage IV, Eq. (3) can be simplified as:

$$-M_{eff} + F\delta = 0 \tag{6}$$

In this stage, at the same temperature, axial forces of the beam with different span-depth ratio are equal, which is determined by yielding stress. Then according to Eq. (6), δ of different beams are equal, but the value of δ / L decreases with L increasing, as shown in Fig. 16.

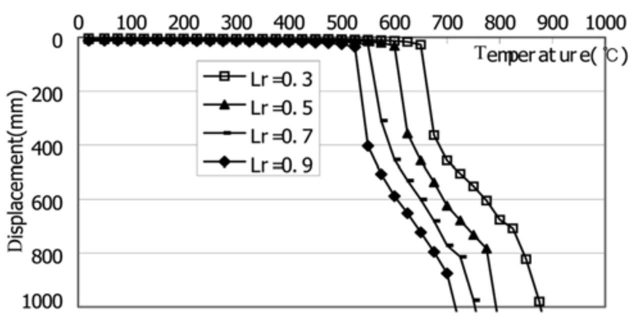

Fig. 14 Deflections of the beam with various load ratios

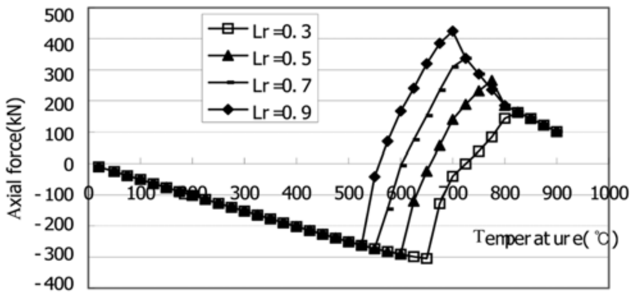

Fig. 15 Axial forces of the beam with various load ratios

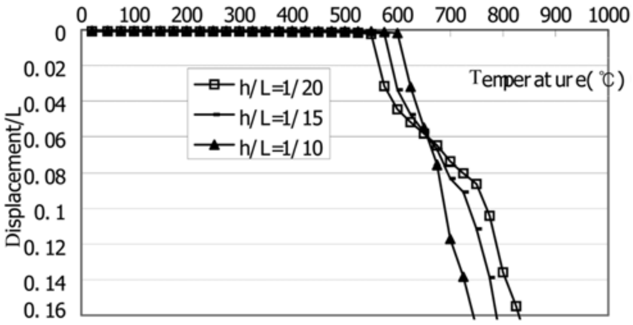

Fig. 16 Deflections of the beam with various depth-span ratios

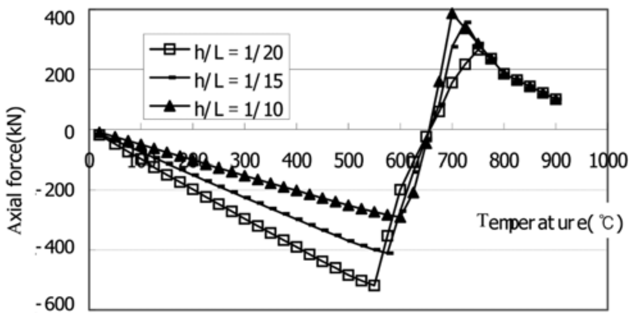

Fig. 17 Axial forces of the beam with various depth-span ratios

2.5 Effects of load type

In this section, three types of applied loads are considered: (1) uniform distributed load; (2) two concentrated load located at $0.3L$ from the ends of the beam; (3) concentrated load at the mid-span of the beam. For the first and the second load types, the deflection curves of the beam are expressed as Eq. (2) and Eq. (1). For the third load type, according to Eqs. (9)~(13) in the companion paper (Li and Guo 2008), the deflection curve of the beam can be expressed as:

$$f(x) = 4\delta \cdot \frac{x^2}{L^2}\left(3 - \frac{4x}{L}\right) \qquad x < L/2 \tag{7}$$

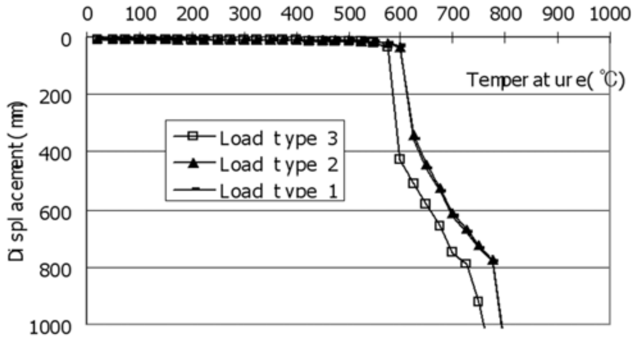

Fig. 18 Deflections of the beam under various load types

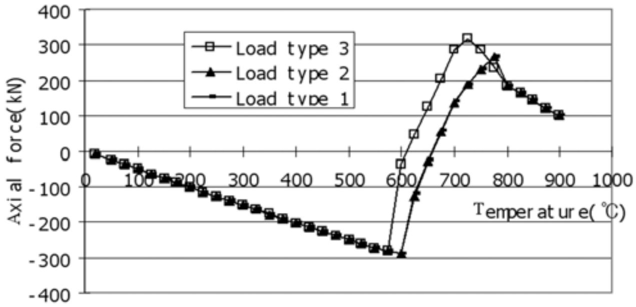

Fig. 19 Axial forces of the beam under various load types

Fig. 20 and Fig. 21 show the developments of deflections and axial forces of the beams with various load types, respectively. It can be seen that the behaviour of the beams with the first and the second load type are similar. But the behaviour of the beam with the third load type is different.

These differences can be explained by that though the load ratios of the beam are the same, the value of M_{eff} in the beam with the third load type is larger than that with the other two load types. Therefore, the beam yields earlier, and the deflection is larger.

At the end of stage II, when F decreases to zero, according to Eq. (3), the larger is M_{eff}, the larger M_{mid} and M_{end} are needed to satisfy the equilibrium equation. While since the lower the temperature, the larger the value of M_{mid} and M_{end}, the temperature when axial force is zero is lower for the beam with the third type than that with the other two load types.

2.6 Effects of non-uniform temperature distribution in the cross-section

In this section, the axial restraint stiffness is assumed to be $0.05k_b$. Fig. 20 and Fig. 21 show developments of deflections and axial forces of two beams, one with uniform temperature distribution, and the other one with non-uniform temperature distribution as shown in Fig. 2.

It can be seen that the beam with uniform temperature distribution yields earlier than the beams with non-uniform temperature distribution, but the difference is small. Therefore, if the temperature distribution in the cross section is not certain, it may be assumed to be uniform and the result of the fire response of the beam will be conservative.

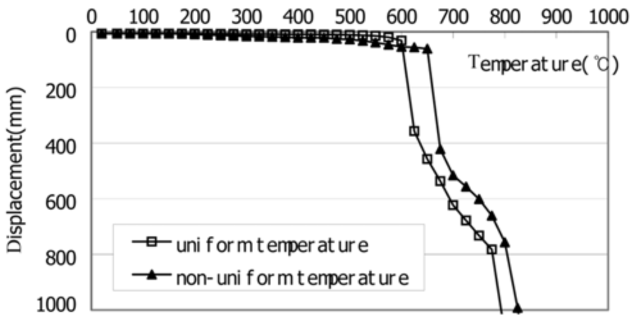

Fig. 20 Deflections of the beam with different temperature distribution

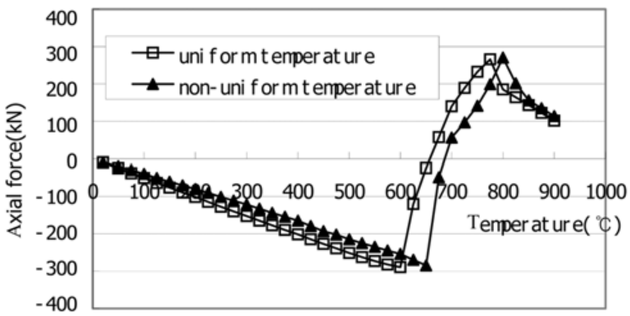

Fig. 21 Axial forces of the beam with different temperature distributio

3. Validation study for restrained steel beams during cooling

Since existing experiments on fire-resistance of steel beam are mainly focused on temperature increasing. There is little available experimental information on restrained beams during cooling. Nevertheless, theoretical investigations on isolated steel beams during cooling have been conducted by El-Rimawi *et al*. (1996) and Baily *et al*. (1996), who produced similar results. To validate the proposed theory (Li and Guo 2008) for analyzing steel beams during cooling, the same beam used by El-Rimawi *et al*. and Baily *et al*. is analyzed. The section of the beam is 356 × 171 × 51UB, and the span is 6.0 m. The temperature of the top flange is assumed to be half of that of the bottom flange. The elastic modulus at ambient temperature is 2.1×10^5 MPa; the yield strength of the steel is 308 MPa. Uniform distributed load applied on the beam is 30.6 kN/m. Fig. 22 compares predicted deflections and those of El-Rimawi *et al*. and Baily *et al*. It can be seen that the deflections predicted with the three approaches are very similar both during heating and cooling.

The results by all the three approaches indicate that though large deflection will be induced for a beam in fire during temperature increasing, most of the deflection will not be recovered in cooling phase.

4. Parametric analysis for restrained steel beams subjected to decreasing temperature

4.1 Effects of maximum temperature T_{max}

A group of restrained steel beams similar to the reference beam introduced in Table 1 are analysed by the method proposed (Li and Guo 2008). When the temperature reaches T_{max}, the temperature begins to descrease. In this analyse, a number of T_{max}, 575°C, 650°C and 700°C, are employed. With variation of T_{max}, developments of deflections and axial forces are shown in Fig. 23 and Fig. 24 respectively and the reversal of deflections and change of the axial forces into tension of the beam are listed in Table 2. It can be seen that the higher is T_{max}, the larger is the deflection reversal and the change in the axial force.

According to the theory in the companion paper (Li and Guo), the contraction force is related to decreasing temperature, as shown in Eq. (8):

$$\Delta F = \alpha L(T_1 - T_2)k_{e,a} \tag{8}$$

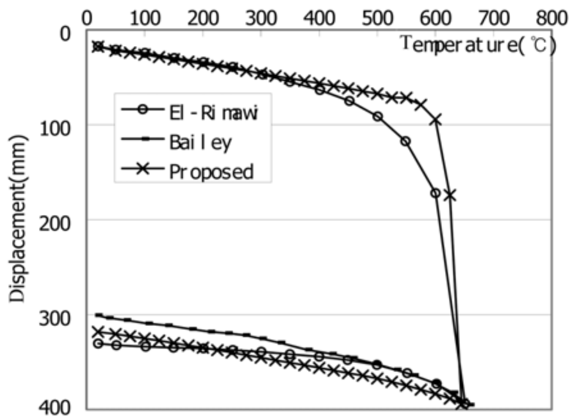

Fig. 22 Comparison of deflections of the beam obtained with various methods during

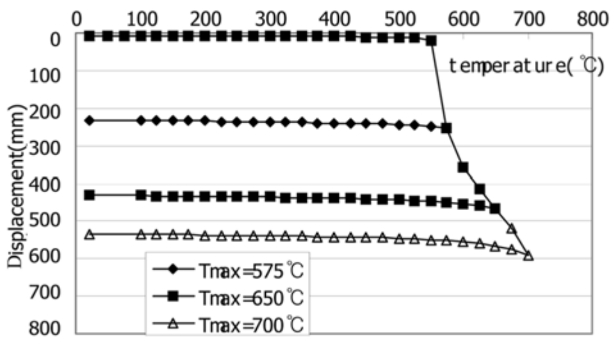

Fig. 23 Deflections of the beam with changing T_{max}

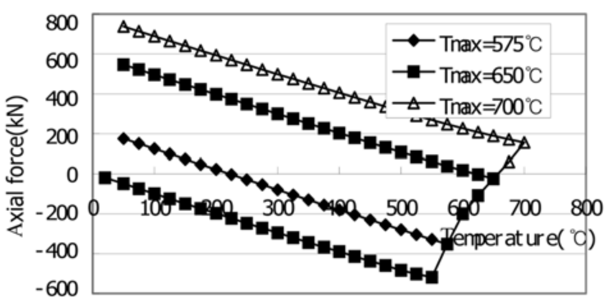

Fig. 24 Axial forces of the beam with different axial restraints stiffness

Table 2 Reversal of deflection and change in axial force in the beam with various T_{max}

	T_{max} = 575°C	T_{max} = 650°C	T_{max} = 700°C
The reversal of the deflection(mm)	21.3	34.3	55.7
The change of axial force(kN)	527.7	569.3	581.8

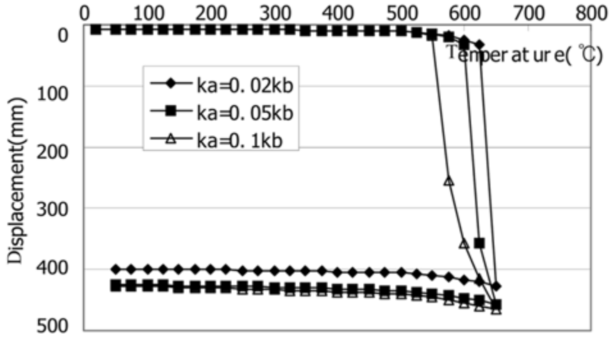

Fig. 25 Deflections of the beam with different axial restraints stiffness

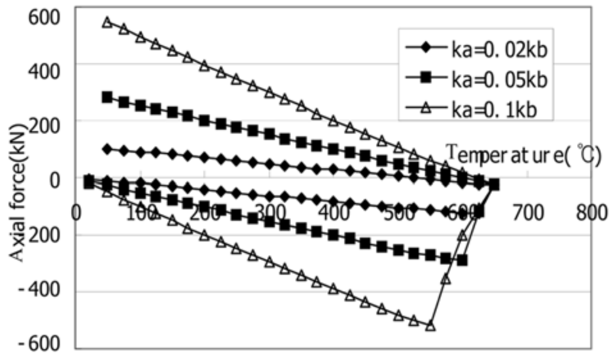

Fig. 26 Axial forces of the beam with different axial restraints stiffness

Table 3 Reversal of deflection and change in axial force in the beam with various axial restraints

	$k_a = 0.02\ k_b$	$k_a = 0.05\ k_b$	$k_a = 0.1\ k_b$
The reversal of the deflection(mm)	27.25	32.44	34.3
The change of axial force(kN)	127.3	304.6	569.3

According to Eq. (8), higher T_{max} induces larger contraction force.

With temperature decreasing, according the companion paper (Li and Guo 2008), elastic modulus of steel recovers, which leads to deflection reversal, as shown in Eq. (9):

$$\delta_{rev,E} = \delta_0 E_0 \left(\frac{1}{E_{T_1}} - \frac{1}{E_{T_2}} \right) \tag{9}$$

where δ_0 is the deflection of the beam at ambient; E_0, E_{T_1} and E_{T_2} are elastic modulus at ambient, temperature T_1 and T_2, respectively.

In addition, the contraction force induces deflection reversal, too. Therefore, higher T_{max} produces larger deflection reversal.

4.2 Effects of axial restraints stiffness

In this analysis, axial restraint stiffness are $k_a = 0.02\ k_b$, $0.05\ k_b$, $0.1\ k_b$. Temperature reaches 650°C and then begins to decrease. Figs. 25 and 26 show developments of deflections and axial forces. Table 3 show defection reversals and changes in axial forces into tension.

It can be seen that the larger the axial restraints stiffness, the larger the change in axial force. It can be reasoned by that the contraction force and axial restraint stiffness are in direct proportion, according to Eq. (8). According to Table 3, larger axial restraint stiffness induces larger deflection reversal, because of larger contraction force.

4.3 Effects of the stiffness of rotational restraints

In this study, the effective rotational stiffness are 0, $0.05EI/L$, $0.1EI/L$ and EI/L. Temperature reaches 650°C and then begins to decrease. Developments of deflections and axial forces of the beams are shown in Fig. 27and Fig. 28 respectively, where γ is the ratio of effective rotational stiffness to EI/L. Deflection reversals and changes in axial forces into tension are listed in Table 4.

It can be seen that for the beam with larger rotational restraint stiffness, deflection reversal is smaller. At ambient temperature, a larger rotational restraint stiffness induces a smaller deflection, δ_0, then according to Eq. (9), a smaller deflection reversal is produced. On the other hand, effets of rotational

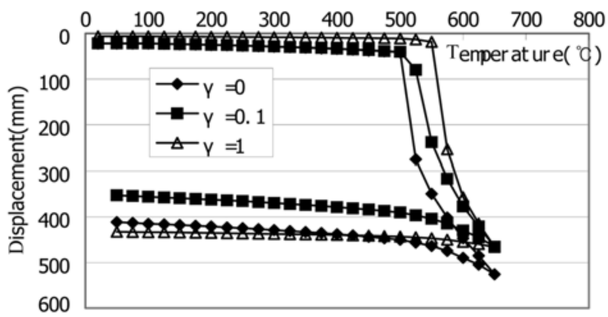

Fig. 27 Deflections of the beam with different rotational restraints stiffness

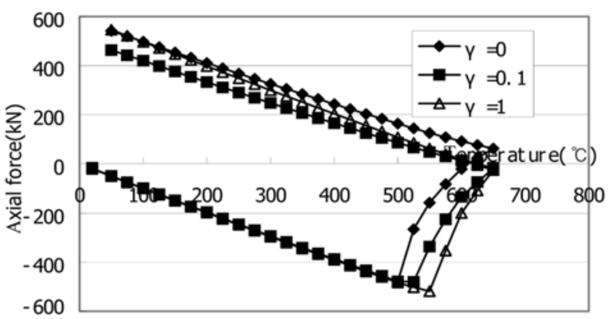

Fig. 28 Axial forces of the beam with different rotational restraints stiffness

Table 4 Reversal of deflection and change in axial force in the beam with various rotational restraints

	$\gamma = 0$	$\gamma = 0.1$	$\gamma = 1$
The reversal of the deflection(mm)	93.2	91.9	34.3
The change of axial force(kN)	479.9	480.7	569.3

restraint stiffness on contraction force is small, which is mainly related to axial restraint stiffness, according to Eq. (8).

5. Conclusions

The theoretical method for analyzing the behavior of restrained steel beams subjected to temperature increasing is validated by experimental measurements. The behavior of the steel beam in cooling phase obtained by the proposed theory (Li and Guo under review) agrees with that by other previous theoretical predictions.

Through the parametric investigation on restrained steel beams subjected to increasing temperature, the following remarks may be drawn as:

1. The catenary action may take effect for a restrained beam subjected to increasing temperature. Increasing the stiffness of the axial restraints, or reducing the depth-span ratio and load ratio can enhance the catenary action.
2. Increasing the stiffness of the axial restraints or load ratio, or reducing the stiffness of the rotational restraints, will result in the beam yields at lower temperature. Increasing the stiffness of axial or rotational restraints, or reducing load ratio, will increase the maximum value of axial compressive force in the beam. Increasing the stiffness of axial or rotational restraints, or load ratio, will increase the maximum value of axial tensile force in the beam in the catenary action.
3. Given the load ratio of the beam is kept constant, the beam supporting uniform load or two concentrated load has better fire-resistant capability than that supporting mid-span concentrated load.
4. If temperature distribution in the cross-section of the beam can't be determined, assuming a uniform temperature distribution will be conservative.

In addition, through the parametric studies on restrained steel beam in cooling phase, the following conclusions may be summarized as:

1. Compared with the large deflection of the beam in heating phase, the deflection reversal of the beam in cooling phase is very small. Axial tensile force in the beam increases with temperature decreasing. When temperature decreases to ambient, tremendous axial tensile force may be induced.
2. The higher is the temperature when begin to decrease, the larger is the deflection reversal and the change in the axial force into tension.
3. Increasing the axial restraint stiffness or reducing the rotational restraint stiffness will increase the deflection reversal. Increasing the stiffness of axial or rotational restraints will increase the change in axial force.

In summary, the effects of the possible factors that influencing the behaviour of restrained steel beam subjected to heating and cooling are listed in Table 5 and Table 6, respectively.

Acknowledgment

The studies presented in this paper are sponsored by the Natural Science Foundation of China through the Outstanding Youth Project (No.59478038). The financial support from NSFC is especially acknowledged.

References

Baily C. G., I. Burgess W. and Plank R. J. (1996), "Analyses of the effect of cooling and fire spread on steel-framed buildings", *Fire Safety J.*, **26**(4), 273-293.

El-Rimawi J. A., Burgess I. W. and Plank R. J. (1996), "The treatment of strain reversal in structural members during the cooling phase of a fire", *J. Constr. Steel Res*, **37**(2), 115-134.

European Committee for Standardization (CEN), DAFT ENV 1993-1-2, Eurocode 3: *Design of steel structures, part 1.2* : *General rules/structural fire design*, 2001.

European Committee for Standardization (CEN), DAFT ENV 1993-1-8, Eurocode 3: *Design of steel structures, part 1.8* : *Design of joints*, 2003.

Huang Z. F. and T K. H. (2002), "Structural response of a steel beam with a frame during a fire", *Proceedings of the Third International Conference on Advances in Steel Structures*, Vol.II, 1111-1118.

International Standard Organization (ISO), ISO834 fire-resistance test-elements of building construction, 1980.

Li G. Q. and Guo S. X. (2008), "Analysis of restrained steel beams subjected to heating and cooling Part I: Theory", *Steel Compos Struct*, **8**(1), 1-18.

Liu T. C. H., Fahad M. K. and Davies J. M. (2002), "Experimental investigation of behaviour of axially restrained steel beams in fire", *J. Constr. Steel Res.*, **58**(9), 1211-1230.

Yin Y. Z., Wang Y. C. (2004), "A numerical study of large deflection behaviour of restrained steel beams at elevated temperatures", *J. Constr. Steel Res.*, **60**(7), 1029-1047.

Yin Y. Z., Wang Y. C. (2005a), "Analysis of catenary action in steel beams using a simplified hand calculation method, Part 1 : theory and validation for uniform temperature distribution", *J. Constr. Steel Res.*, **61**(2), 188-211.

Yin Y. Z., Wang Y. C. (2005b), "Analysis of catenary action in steel beams using a simplified hand calculation method, Part 2 : validation for non-uniform temperature distribution", *J. Constr. Steel Res.*, **61**(2), 213-234.

BU